Dynamic myocardial CT perfusion imaging

Assen ,van, Marly; Pelgrim, Gert Jan; Vliegenthart, Rozemarijn

Published in:
CT of the heart

DOI:
10.1007/978-1-60327-237-7

Dynamic Myocardial CT Perfusion Imaging

63

Marly van Assen, Gert Jan Pelgrim, and Rozemarijn Vliegenthart

Several noninvasive imaging techniques are available for the evaluation of myocardial perfusion. Nuclear techniques are positron emission tomography (PET) and single-photon emission computed tomography (SPECT). PET is the current gold standard for quantitative evaluation of myocardial perfusion, while SPECT is the most commonly used imaging method for myocardial ischemia [1]. Cardiac magnetic resonance (MRI) perfusion imaging has, however, shown better accuracy for the detection of myocardial perfusion defects [2].

In a meta-analysis involving 11,826 patients [3], myocardial perfusion evaluation with PET had a higher sensitivity for myocardial ischemia than evaluation with SPECT, 92.6% compared to 88.3%, respectively. There was no significant difference between the specificity of PET and SPECT, 81.3% compared to 76.0%. Jaarsma et al. [1] showed in a recent meta-analysis (17,901 patients) a pooled sensitivity of 84%, 88%, and 89% for PET, SPECT, and MRI, respectively, with a pooled specificity of 81%, 61%, and 76%. They concluded that both PET and MRI showed higher diagnostic accuracy than SPECT.

None of the abovementioned techniques allow simultaneous anatomical and functional evaluation of coronary artery disease (CAD). Computed tomography (CT), however, is able to evaluate both with state-of-the-art imaging techniques. Coronary CT angiography (CCTA) is often used for noninvasive evaluation of coronary anatomy, yielding a very high sensitivity and negative predictive value close to 100% [4]. Combining CT myocardial perfusion imaging (CTMPI) with CCTA allows for anatomical and functional evaluation of CAD using a single modality and examination.

Dynamic CTMPI uses multiple acquisitions to capture the first pass of contrast medium during its wash in and washout through the myocardium; this is in contrast to static CT perfusion imaging which only shows contrast distribution across the myocardium at a single point in time [5–8].

The main advantage of dynamic CTMPI is the potential of quantitative analysis of myocardial blood flow (MBF), myocardial blood volume (MBV), and other perfusion-related parameters directly from the CT images, for both the whole heart and for individual myocardial segments. Static CT does not provide a quantitative measure of perfusion but a relative map of single-time-point myocardial contrast distribution. Quantification of MBF could especially improve the detection of ischemia in patients with three-vessel disease because this approach relies on absolute values of MBF rather than on the differences between normal and ischemic myocardium. Also, subtle subclinical decreases in MBF can be detected by quantifying perfusion, while not yet visible as gross perfusion defects [9].

CTMPI was first studied in a number of animal studies. Studies in pigs and dogs showed that dynamic CTMPI was able to determine accurate MBF values, using 16- or 64-multidetector CT (MDCT) during rest and stress. CTMPI-determined semiquantitative and quantitative MBF values as well as rest/stress MBF ratios were shown to have a high correlation with microsphere-derived MBF [10–12]. In studies by Mahnken et al. [13] and Bamberg et al. [14], a dual-source CT (DSCT) system with alternating table positions ("shuttle mode") allowed for whole heart imaging in pigs, with a total coverage of 73 mm compared to 38 mm using only one table position. DSCT scanners have an improved temporal resolution due to

M. van Assen
Department of Radiology, University of Groningen, University Medical Center Groningen, Groningen, The Netherlands

Department of Radiology and Radiological Science, Division of Cardiovascular Imaging, Medical University of South Carolina Charleston, SC, USA
e-mail: vanasse@musc.edu

G. J. Pelgrim
Department of Radiology, University of Groningen, University Medical Center Groningen, Groningen, The Netherlands

R. Vliegenthart (✉)
Department of Radiology, University of Groningen, University Medical Center Groningen, Groningen, The Netherlands

Department of Radiology and Radiological Science, Division of Cardiovascular Imaging, Medical University of South Carolina Charleston, SC, USA
e-mail: r.vliegenthart@umcg.nl

U. J. Schoepf (ed.), *CT of the Heart*, Contemporary Medical Imaging, https://doi.org/10.1007/978-1-60327-237-7_63

the use of two X-ray sources, resulting in the possibility to scan a slab in less than 150 ms. Using DSCT in shuttle mode, they were able to show the hemodynamic effect of a coronary stenosis with dynamic CTMPI in stress phase and concluded that CT-determined MBF measurements could differentiate ischemic from nonischemic myocardium. However, MBF was underestimated compared to microsphere-determined MBF. Rossi et al. [15] showed that dynamic dual-source CTMPI is able to distinguish regions with reduced MBF during stress phase imaging with a good correlation with FFR measurements. They used a higher dose of adenosine as a stressor agent, 500 μg/kg/min, compared to Bamberg et al. and Mahnken et al. who used 140 μg/kg/min and 240 μg/kg/min, respectively. Contrast agent was injected directly into the pulmonary vein, whereas in the studies of Bamberg et al. and Mahnken et al., the contrast agent was injected into a peripheral vein. Rossi et al. [15] found higher MBF values than the studies of Bamberg et al. and Mahnken et al. 2.68 (2.31–2.81) ml/g/min compared to 1.10(±0.25) ml/g/min and 117.4(±18.6) ml/100 ml/min in nonischemic myocardium during stress phase, possibly caused by the differences in experimental setup. Apart from animal validation studies, in recent years a number of patient studies have been performed, evaluating the feasibility of CTMPI in a clinical setting. These studies will be discussed later in this chapter, after discussing the technical issues in CTMPI.

Technical Information

Heart Coverage

The accuracy of dynamic CTMPI logically depends on the heart coverage of the available CT systems. The first systems used for dynamic CTMPI in clinical patients were DSCT systems. Second-generation DSCT scanners allow coverage of most of the left ventricle (7.3 cm) using a shuttle mode in systolic phase. The shuttle mode consists of back-and-forth table movements alternated with sequential scanning to cover the left ventricle in two separate scans, which are later combined to reconstruct one image. Third-generation DSCT systems have wider detectors compared to second-generation scanners, enabling whole heart imaging in systolic phase with a total range of 10.2 cm. Although the shuttle mode enables the coverage of a larger portion of the heart, the movement between the two table positions lowers the temporal sampling rate, especially at high heart rates. A low temporal sampling rate results in a decrease in information on in- and outflow of contrast medium in the myocardium, the so-called first-pass perfusion, and could thereby cause inaccurate estimation of MBF values [16]. Another problem introduced by the moving table positions is the possibility of motion artifacts, decreasing the accuracy of the measurements. Single-tube multi-detector CT (MDCT) scanners with 256 or 320 detector rows cover 8 and 16 cm, respectively. Wide detector coverage enables (nearly) full left ventricle imaging with a stationary table position, allowing a higher temporal sampling rate. These CT systems offer the same or even more coverage compared to DSCT scanners without the disadvantage of table movement in shuttle mode, so far however at the disadvantage of higher radiation dose.

Cardiac Phase for Acquisition

Image acquisition is possible in systolic or diastolic phase. Motwani et al. [17, 18] studied the effect of systolic and diastolic acquisition on quantitative MRI perfusion imaging and reported higher diastolic stress MBF values compared to systolic stress MBF. However, diagnostic accuracy for myocardial ischemia was similar for systolic and diastolic acquisition. There are several important advantages for CT acquisition during the systolic phase. Firstly, the heart is contracted during systole, with maximal contraction at end systole, resulting in a smaller total heart volume, in particular a shorter basal-apical length. Thus, the range that needs to be covered for visualizing the entire heart within one scan cycle is reduced. Because of the maximal contraction, the myocardium is thicker in systole and allows for easier delineation during analysis. Secondly, although the systolic phase is shorter than the diastolic phase, the systolic phase has a constant duration (200 ms approximately) independent of heart rate and is less sensitive to arrhythmia. Thirdly, image acquisition during the systolic phase results in a lower-contrast dose in the left ventricle and, thus, reduces beam-hardening artifacts [8, 18, 19].

Radiation Dose

Cardiac imaging is a major contributor to the average population medical radiation exposure [7, 20]. Dynamic CTMPI is associated with a relatively high radiation dose since it requires multiple scan acquisitions during the first pass of contrast.

Effective radiation doses between 5 and 13 mSv, with an average dose of 9.2 mSV, have been reported for dynamic CTMPI procedures (Tables 63.1 and 63.2). Cardiac patients often undergo multiple imaging procedures in their life, increasing their cumulative radiation exposure [5, 6, 20]. One particular advantage of CT, however, is that both coronary stenosis and resulting myocardial ischemia can be evaluated with one imaging modality. In view of the significant reduction in radiation dose with newest CT systems for coronary imaging, the total radiation dose of CTA plus CTMPI does not need to exceed 10 mSv [39–41].

The effective radiation dose of CT perfusion procedures is within the range of nuclear perfusion imaging procedures. SPECT perfusion studies show radiation doses of 6.6 mSv for stress-only imaging and 11.3 mSv for both rest and stress phase imaging. PET perfusion studies need a radiation ranging from 2.4 mSv to 13.5 mSv [42].

Table 63.1 Dynamic CT myocardial perfusion patient studies using visual analysis

Study	Year	Number of patients	CT scanner	Radiation dose (mSv)	Reference	Analysis	Sens	Spec
Yang [21]	2016	72	Second-generation DSCT	7.8	ICA + FFR	Territory	79	91
Baxa [22]	2015	27	Second-generation DSCT	8.9	ICA	Territory	97	95
						Segmental	98	96
Weininger [23]	2012	10	Second-generation DSCT	12.8	MRI	Segmental	86	98
					SPECT	Segmental	84	92
Wang [24]	2012	30	Second-generation DSCT	9.5	CCTA + SPECT SPECT	Segment	100	76
Bastarrika [25]	2010	10	Second-generation DSCT	18.8	MRI	Segmental	86	98

Note: *DSCT*, dual-source *CT*; *MDCT*, multi-detector CT; *ICA*, invasive coronary angiography; *FFR*, fractional flow reserve; *MRI*, cardiac magnetic resonance; *SPECT*, single-photon emission CT

Radiation dose reduction techniques in CTMPI show promising results. Performing a scan only in stress instead of both in rest and stress phase considerably reduces the radiation dose. A rest/stress phase combination, for example, in MR and PET perfusion imaging, is normally performed to acquire information about the reversibility of a perfusion defect, which could help to differentiate ischemia from myocardial infarction; see Fig. 63.1. However, in symptomatic patients without history of myocardial infarction, the probability of a persistent perfusion defect is low. In these patients, the main reason for CT imaging is to detect hemodynamically significant CAD, where presence of coronary stenosis is combined with evaluation of ischemia in the same vascular territory. Danad et al. [43] showed that the stress MBF value has a higher diagnostic accuracy than an index parameter comparing rest and stress acquisitions acquired using PET. This implies that a single MBF measurement during stress phase could be sufficient to evaluate the significance of a coronary stenosis. Delayed enhancement scans are used to detect myocardial scarring and also to determine the difference between ischemic and infarcted myocardium in patients with history of heart disease. Delayed enhancement CT falls outside the scope of the current chapter.

Another option to reduce radiation dose is by lowering the tube voltage in patients with a normal body mass index (BMI) from 100 kVp to 80 or 70 kVp [44]. This reduces the radiation dose up to 40% compared to 100 kVp, where 100 kVp can be reserved for patients with a BMI higher than 25 kg/m [2, 44]. Kim et al. [39] showed that automatic dose-modulation techniques combined with a decreased scan duration during the first pass limit the radiation dose significantly without compromising the image quality. Of course, when decreasing scan duration, it is important that the entire upslope of the contrast at first pass is acquired. Iterative reconstruction techniques can be used to compensate the loss of image quality when using a lower-tube current [45].

Despite the developments in dose reduction techniques, CTMPI procedures still yield a relatively high radiation exposure compared to other CT examinations. Patient-tailored CTMPI protocols are essential to reduce unnecessary radiation exposure.

Temporal Sampling Rate

The temporal resolution of dynamic CTMPI needs to exceed the timescale of the fastest process observed; otherwise, the perfusion parameters may be incorrect and most likely be underestimated. The fastest process in contrast medium kinetics is typically the vascular transit time. For example, in dynamic brain perfusion imaging, the minimal temporal sampling rate is 2 s. Several articles imply that a low temporal sampling rate in cardiac imaging, for example, in shuttle mode, leads to underestimation of the MBF in dynamic CTMPI [16, 46]. Temporal sampling rates of one acquisition every second heartbeat for low heart rates, up to one acquisition per four heartbeats at high heart rates (which are common in stress situations), are reported using a DSCT system in shuttle mode [13, 16, 46]. These temporal sampling rates may be insufficient to accurately capture the first-pass contrast enhancement curve.

Patient Preparation and Scanning Protocol

There are a number of points to consider in patient preparation. Patients should not use caffeine (coffee, tea, bananas, chocolate, etc.) for preferably 24 h or more before the examination, because of the interfering effects of caffeine on the effectiveness of the stressor agent. During the CCTA, beta-blockers may be needed to lower the heart rate in order to optimize image quality. Some studies have found that the use of beta-blockers may have a negative effect on the detection of myocardial ischemia by increasing the diastolic perfusion time [47, 48]. Sublingual nitrates, also commonly used in CCTA, have been shown to decrease the ischemic area on perfusion images [47].

At this time, CTMPI is not yet clinically used apart from certain centers in Asia. The exact position of CTMPI in the work-up of CAD is still under investigation. When considering implementing CCTA with CTMPI, it is still a point of debate whether CCTA or CTMPI should be the first in the examination order. In patients with a high probability or known CAD (after stenting or bypass grafting) in whom myocardial ischemia is likely, CCTA can be performed after the stress CTMPI procedure; see Fig. 63.2. This eliminates

Table 63.2 Dynamic CT myocardial perfusion patient studies using (semi)quantitative analysis

Study	Year	Number of patients	CT scanner	Radiation dose (mSv)	Reference	Analysis	Parameter	Model used	Sens	Spec	Cutoff (ml/100 ml/min)
Tanabe [26]	2016	53	256 row MDCT	10.5	SPECT	Segment	MBF	Singular value decomposition	80	86	0.92 mL/g/min
					MRI				82	87	0.98 mL/g/min
Wichmann [27]	2016	71	Second-generation DSCT	8.2	Visual CT	Patient	MBF (3 territories)	Two-compartment model + upslope (Siemens)	100	100	88
							MBF (2 territories)		81	91	15
							MBF (1 territory)		76	87	109
							MBV (3 territories)		100	88	16
							MBV (2 territories)		75	91	136
							MBV (1 territory)		86	45	20
Wichmann [28]	2015	137	Second-generation DSCT	643.8 (mGy. Cm)	CCTA	Territory	MBF	Patlak (Siemens)	82	81	103
							MBF ratio		91	93	0.71
Bamberg [29]	2014	31	Second-generation DSCT	11.1	MRI	Territory	MBF	Patlak (Siemens)	100	75	88
						Segment			78	75	
						Patient			100	75	
Ebersberger [30]	2014	37	Second-generation DSCT	9.6	SPECT	Segment	MBF	Patlak (Siemens)	86	96	Individual thresholds
							MBV		81	96	
Kono [31]	2014	42	Second-generation DSCT	9.4	ICA + FFR	Territory	MBF	Patlak (Siemens)	89	48	103
							MBF ratio		98	70	0.85
Rossi [32]	2013	80	Second-generation DSCT	9.4	ICA	Territory	MBF	Patlak (Siemens)	88	90	78
						Patient			90	88	
Huber [33]	2013	32	256 row MDCT	9.5	ICA + FFR	Territory	MBF	Linear fit+upslope method	76	100	1.64 ml/g/min
							Upslope	–	83	88	
Greif [34]	2013	65	Second-generation DSCT	9.7	ICA + FFR	Territory	MBF	Patlak (Siemens)	95	74	75
						Patient			97	66	
So [35]	2012	26	64-MDCT	9.7	SPECT		MPR	Distributed parameter model	95	35	2.5 ml/g/min
							MVR		97	24	1.4
Bamberg [36]	2011	33	Second-generation DSCT	10	ICA + FFR	Territory	MBF	Patlak (Siemens)	93	87	75
						Segment			91	98	
						Patient			95	64	
Ho [37]	2010	35	Second-generation DSCT	9.2	ICA	Segment	MBF	Patlak (Siemens)	83	78	–
Kido [38]	2008	14	16- MDCT	–	QCA	Territory	MBF	Patlak plot analysis	73	81	1.5 ml/g/min
					SPECT				88	79	

Note: *DSCT*, dual-source CT; *MDCT*, multi-detector CT; *CCTA*, coronary CT angiography; *ICA*, invasive coronary angiography; *FFR*, fractional flow reserve; *QCA*, quantitative coronary angiography; *MRI*, cardiac magnetic resonance; *SPECT*, single-photon emission CT; *MBF*, myocardial blood flow; *MBV*, myocardial blood volume; *MPR*, myocardial perfusion reserve; *MVR*, myocardial volume reserve

the influence of beta-blockers and nitroglycerin on the stress CTMPI acquisition. In view of the relatively high radiation dose of CTMPI, in less-than-high probability patients it would be preferable to start with CCTA, in order to avoid unnecessary radiation dose in the case of no stenosis. This, however, would require direct reading of CCTA, which may not be logistically feasible. An advantage could be that beta-blockers given for CCTA may, if CTMPI follows, result in lower maximum heart rate during stress, which can lead to higher temporal sampling rate.

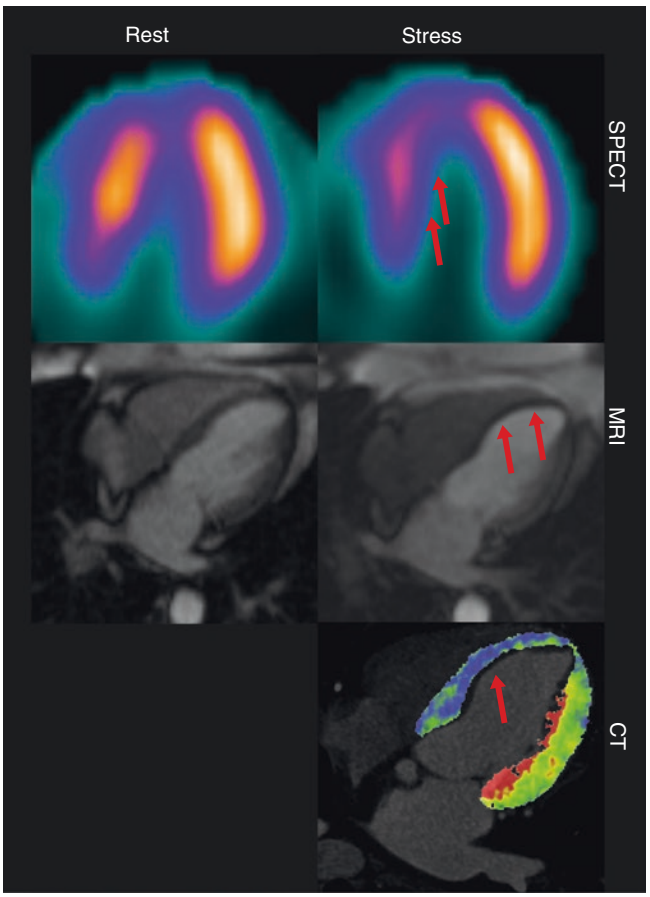

Fig. 63.1 Rest and stress perfusion images made by SPECT and MRI. For dynamic CTMPI stress imaging only could be sufficient

Compared to normal CCTA equipment, an additional infusion pump may be needed for the administration of the stressor agent and an additional intravenous catheter unless contrast medium and stressor are administered into the same arm such as in the case of regadenoson. Patients should be observed continuously during the CTMPI procedure with a 12-lead ECG and a blood-pressure monitor.

An optional, delayed acquisition (10–15 min after last contrast bolus) can be considered in order to differentiate between ischemic and infarcted myocardium in patients with known CAD. With a delayed enhancement (DE) scan, infarcted myocardium can be identified owing to the delayed in- and outflow of contrast of infarcted myocardium. This results in increased HU values in DE imaging. For this DE scan, administration of contrast medium beyond that administered during the stress or rest phase is not needed. However, DE scan acquisition might not be needed for the differentiation between ischemia and infarction. Bamberg et al. [29] showed that myocardial blood volume (MBV) is decreased in infarcted myocardium compared to ischemic myocardium, while MBF is reduced in both conditions. Also, actual MBF cutoff values may allow distinguishing between ischemia and infarction, as MBF in infarcted segments was found to be lower than in merely ischemic segments according to a study comparing CTMPI to MRI and SPECT [26].

Image Analysis

Analysis of dynamic CTMPI images is based on the distribution of contrast medium throughout the myocardium. The distribution of iodine contrast medium can be described in two time-intensity curves. The tissue attenuation curve (TAC) describes the concentration of contrast medium in the myocardium over time, and the arterial input function (AIF) describes the concentration of contrast medium in the supplying artery (assessed at aorta or left ventricle).

Assessment of myocardial perfusion can be performed visually, semiquantitatively, or quantitatively. It should be

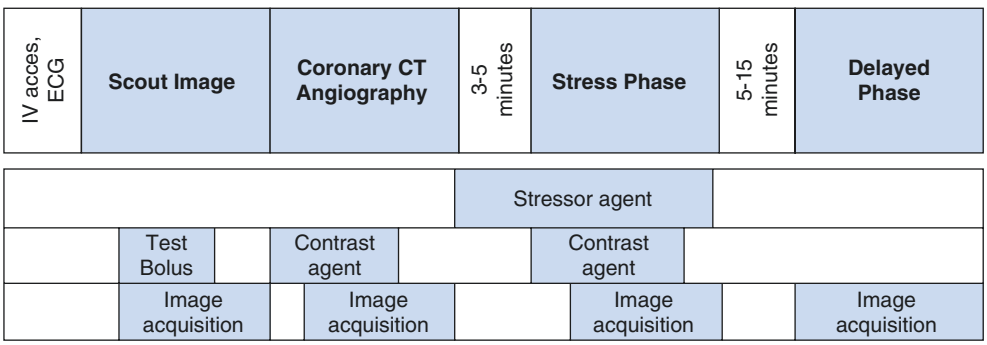

Fig. 63.2 Schematic representation of complete cardiac evaluation protocol, including anatomical (CCTA) and functional (dynamic CTMPI) evaluation. A third, optional scan is the delayed enhancement scan for the detection of infarcted myocardium

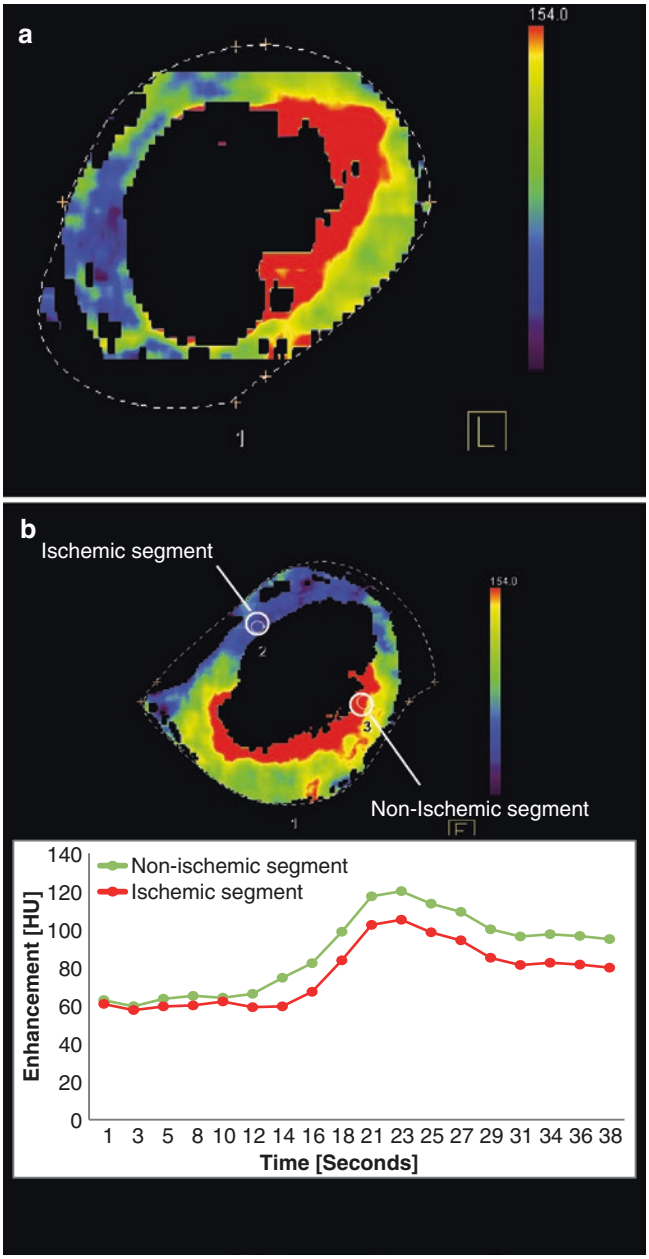

Fig. 63.3 (**a**) Color-coded perfusion map of myocardial blood flow. (**b**) The color-coded map is based on quantitative data. Regions of interest (white circles) represent a tissue attenuation curve (TAC) specific for that area

noted that, in contrast to static CTMPI, visual analysis of dynamic CTMPI is often based on quantitative data, by creating color maps based on MBF data; see Fig. 63.3. In this chapter qualitative analysis refers to visual analysis of CTMPI data without the use of any quantitative measure and may include the visual assessment of color-coded maps.

Myocardial perfusion can be assessed on a segment, territory, or patient basis. For segmental analysis, the 16-segment American Heart Association model is recommended [49]. This segmentation uses three imaging slices at basal, mid-cavity, and apical level. The basal and mid-cavity slices are each divided into six equal segments, whereas the apical slice is divided into four equal segments. The apex (segment 17) is often not taken into account for perfusion analysis because the limited scan width of most scanners does not allow the apex to be imaged [49]. Segmental CT perfusion analysis can be compared to other perfusion modalities such as MRI, PET, or SPECT. Perfusion analysis of vessel territories is based on a three-vessel division, namely, the left descending artery (LAD), the right coronary artery (RCA), and the circumflex artery (LCx) territory. Perfusion parameters are calculated per segment, after which multiple segments are averaged to represent a territory. Segments 1, 2, 7, 8, 13, and 14 are assigned to the LAD territory; segments 3, 4, 9, 10, and 15 are assigned to RCA territory; and segments 5, 6, 11, 12, and 16 are generally assigned to the LCx territory, depending on coronary dominance [49]. Anatomic variations in supplying arteries, however, may pose a problem. Territory analysis can be additionally compared with methods which analyze CAD severity on vessel level such as ICA and FFR methods. With nuclear modalities and MRI, it is also possible to analyze perfusion on a territory level.

For clinical purposes it is important to know whether a patient has myocardial ischemia and is in need of an intervention. Therefore, per-patient analysis is important for clinical diagnostics, while segment- and territory-based analyses are mostly used to validate the technique.

Qualitative, Visual Analysis

Qualitative analysis of dynamic CTMPI data can be done by visually inspecting the enhancement of myocardial tissue during the first pass of iodine contrast on dynamic series. Myocardium with reduced perfusion is hypo-attenuated and enhances later compared to normally perfused myocardium on CTMPI scans. Hypo-attenuation can in principle indicate both ischemic and infarcted myocardium. Visual analysis of dynamic CTMPI images is often done by analysis of color-coded maps; see Fig. 63.4. It is important to realize that these color-coded maps are actually based on quantitative information of myocardial perfusion. In contrast to SPECT, which primarily allows evaluation of relative perfusion of myocardial areas within a patient, the color map based on dynamic CTMPI represents actual MBF values, which allows assessment of globally reduced perfusion in three-vessel disease [50]. Below we describe the quantification of the underlying perfusion parameters.

Semiquantitative Analysis

Semiquantitative parameters can be derived from the TAC curves. The upslope method, in which the upslope of the TAC

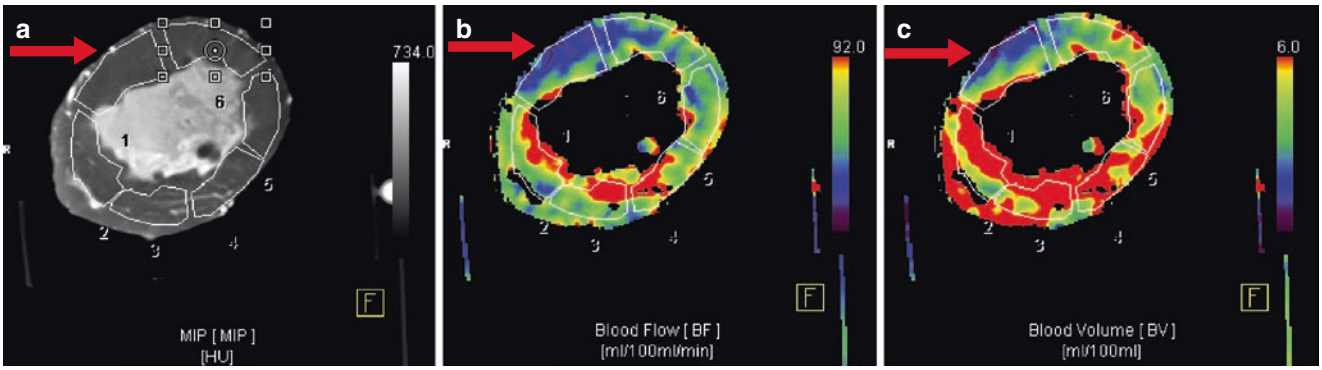

Fig. 63.4 (**a**) Mid ventricular slice of a dynamic CTMPI of a porcine heart with corresponding color-coded map representing (**b**) myocardial blood flow (MBF) in ml/100/ml/min and (**c**) myocardial blood volume (MBV) in ml/100 constructed with Volume Perfusion CT (VPCT) myocardium software (MMWP VA41A, Siemens). The AHA segmentation is projected onto the CT images. The red arrows point two the perfusion defects present in both hearts corresponding to both a decrease in MBF as in MBV

curve is taken as an indirect measure of perfusion, is a popular method to analyze CTMPI data. The upslope is calculated by making a linear fit of the upslope of the TAC curve. The main advantage of using the upslope is the possibility of shortening the scan time and thereby reducing the radiation dose since only knowledge of the wash in of contrast medium is required. For the upslope method, timing of the scan window is highly important. When the entire upslope of the curve is not included, the upslope method becomes inaccurate.

With the upslope method, MBF can be estimated with the following equation:

$$\mathrm{MBF} = \frac{\mathrm{Maxupslope}(\mathrm{TAC})}{\mathrm{Maximum}(\mathrm{AIF})} \qquad (63.1)$$

where the maximum upslope of the TAC (Maxupslope(TAC)) is divided by the maximum value of the AIF curve (Maximum(AIF)); see Fig. 63.5.

The upslope method accurately estimates MBF if the maximum slope of the TAC curve is within the mean tissue transit time, the time that a certain blood volume spends in the myocardium. In stress phase the mean tissue transit time is decreased, more so in normal myocardium than in ischemic myocardium. This decrease can cause an underestimation of MBF [51]. Another issue arising with the use of the upslope method is the inaccuracy of the AIF and TAC in the case of low temporal sampling rates. When temporal sampling rate is too low, the AIF and TAC consist of only a few measurement points during upslope, and important characteristics of both AIF and TAC can be missed.

Other semiquantitative parameters are peak enhancement, time to peak, and area under the curve, all derived from the TAC. From these semiquantitative parameters, the upslope is the most commonly used in MRI studies on semiquantitative analysis of myocardial perfusion [52–54].

Quantitative Analysis

There are several methods to perform true quantitative analysis of perfusion data, based on the AIF and TAC; see Fig. 63.6. Of these methods, the model-dependent deconvolution method is most frequently used in recent literature on cardiac and brain MRI perfusion analysis [51, 55]. Considering that the contrast media currently used in MRI (gadolinium) and CT (iodine) behave according to the same kinetic principles, the same approach can be used [51, 55, 56].

Quantitative CT perfusion analysis using model-dependent convolution can be divided in two phases. First, the signal-time curves (AIF and TAC) should be transformed into iodine concentration-time curves [10, 51]. In comparison with MRI, this is relatively easy for CT data since the change in HU values is linearly related to the iodine concentration [10].

Thus, the iodine concentration is proportional to the signal enhancement:

$$c(t) = k * \left(\mathrm{HU}(t) - \mathrm{HU}_0\right) \qquad (63.2)$$

In this formula, $c(t)$ is the iodine concentration over time, and HU_0 is the baseline HU value (i.e., before iodine injection). K is an unknown scale constant that is automatically corrected for during the second phase, assuming that k is tissue independent [51].

Second, a model-dependent deconvolution approach can be used to describe the perfusion process in the myocardium. This convolution theory-based approach is similar to deconvolution methods and models used in cardiac MRI studies [51, 57]. The iodine concentration in the myocardium over time is related to the iodine concentration in the supplying artery, convoluted ($\otimes$) by an impulse response

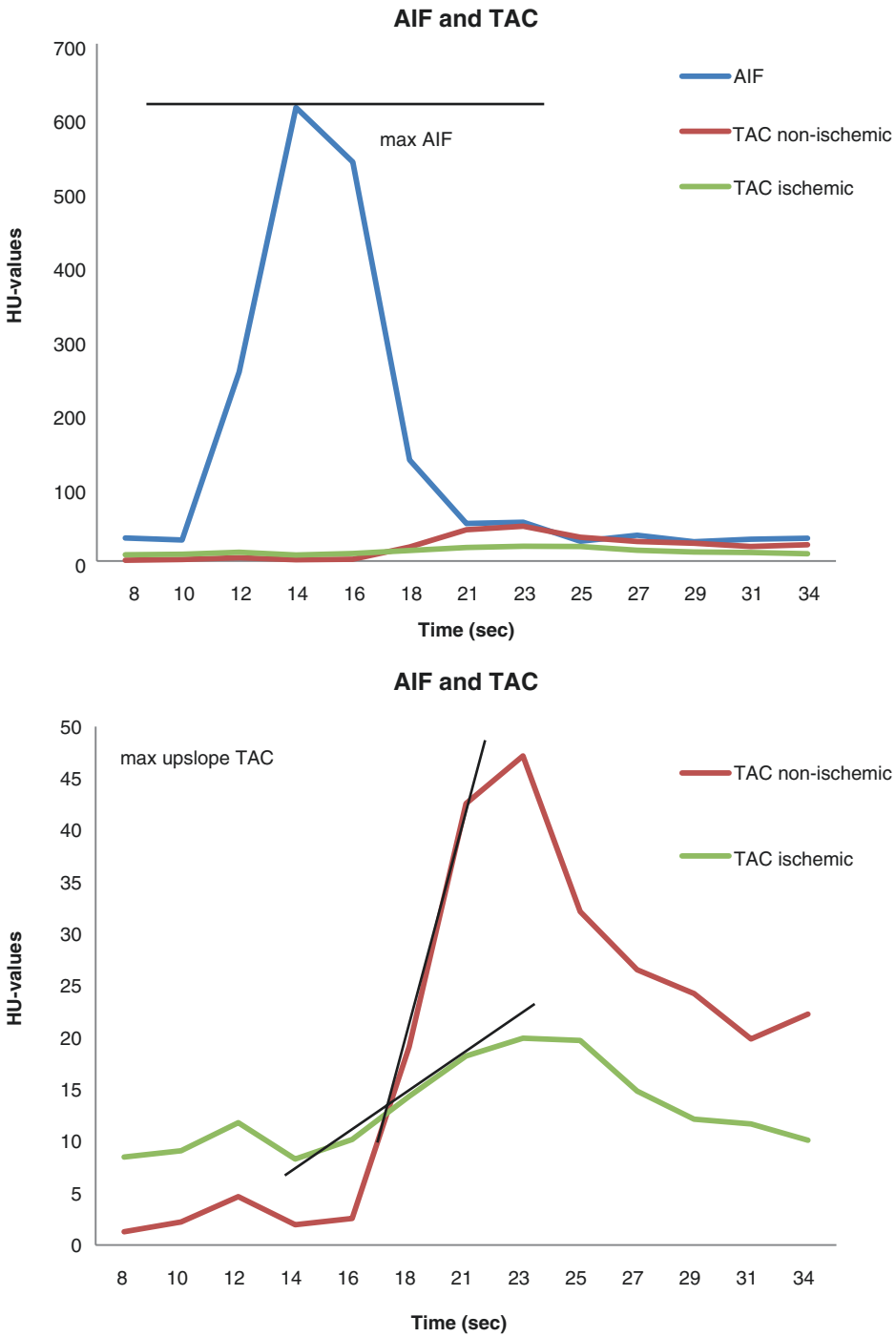

Fig. 63.5 The left figure shows the arterial input function (AIF) and the tissue attenuation curves (TAC) of a nonischemic segment and an ischemic segment. The ischemic segment shows a decreased inflow of contrast compared to the nonischemic segments. On the right is an extended graph showing the TAC in more detail. The maximum AIF value and maximum upslope of the TAC curve, used to calculate the myocardial blood flow, are indicated by black lines

function (IRF). This relation is described by the following equation [55, 56, 58]:

$$\mathrm{TAC}(t) = \mathrm{MBF} * \mathrm{AIF}(t) \otimes \mathrm{IRF}(t) \qquad (63.3)$$

where TAC(t) is the tissue attenuation curve over time (seconds) in HU values, MBF is the myocardial blood flow, AIF(t) is the arterial input function over time in HU values, and IRF(t) is the impulse response function over time.

If IRF(t) is known, the TAC can be obtained as a summation of adjusted IRFs; see Fig. 63.7. In dynamic CTMPI AIF and TAC are known parameters, measured from the CT images, whereas IRF(t) is the unknown parameter. The reversed process to reconstruct the IRF(t) is called deconvolution. The main issue with a deconvolution approach is that in contrast with convolution, deconvolution cannot give a unique solution because there are multiple IRF(t) estimations possible that would result in the same TAC(t)

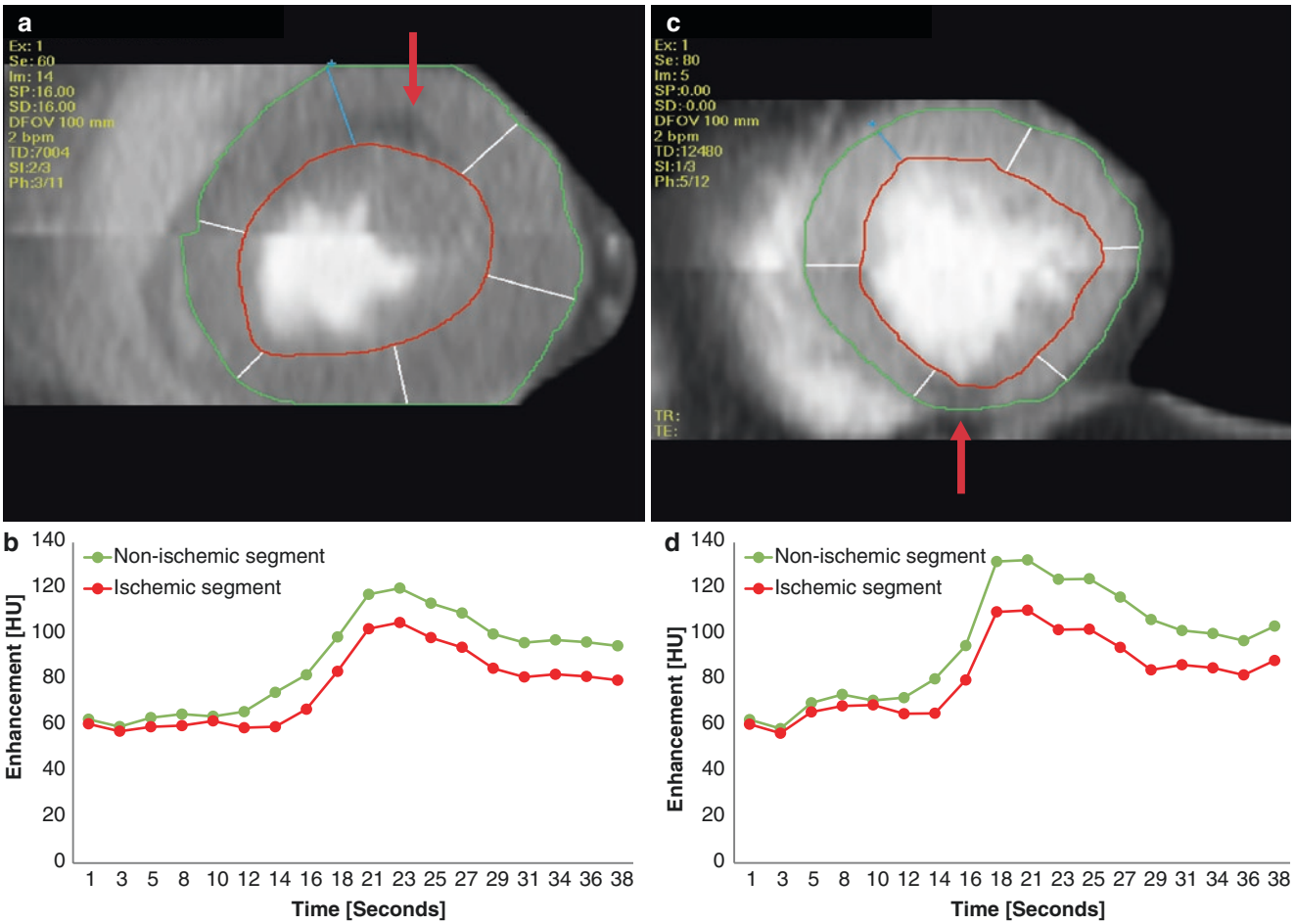

Fig. 63.6 (**a**–**c**) both show a midventricular slice of a dynamic CTMPI scan with a segmental overlay. A perfusion defect is visible in both scans (red arrows). (**b**–**d**) give the corresponding tissue attenuation curve (TAC) of a nonischemic segment without the perfusion defect (green) and of the ischemic segment with a perfusion defect (red) during multiple time points, where the TAC of the ischemic segments in both scans shows a decreased enhancement

or even a better approximation of the TAC(t). This problem is solved in model-dependent deconvolution by determining a generic model to represent the IRF(t) and setting predefined boundaries for the estimated parameters describing this model [55].

In the model-dependent deconvolution method, a tracer-kinetic model is assumed to represent IRF(t), after which the model parameters can be optimized to best fit Eq. (63.3) to the measured TAC data [51, 55, 56]. From the fitted model of the estimated IRF(t), the MBF value can be derived using Eq. 63.3, with known TAC(t), AIF(t), and IRF(t).

Convolution and deconvolution techniques are difficult because noise in either the AIF or TAC data can influence the model optimization and result in an unstable solution for IRF(t) and unreliable MBF values [58]. Noise in CTMPI data can be caused, for example, by inaccurate HU values, measured during different cardiac phases. Reducing noise is therefore an important issue in dynamic CTMPI.

Tracer-Kinetic Models

A wide variety of tracer-kinetic models can be used to represent IRF(t). Each of these models has its merits and limitations; the optimal model for CTMPI analysis has yet to be determined.

The microcirculation of the myocardium is depicted in Fig. 63.8a. Iodine is considered an extravasating contrast medium. The contrast medium distributes across the intravascular space and the extracellular extravascular space, both defined by volume and transit time parameters. High-order perfusion models try to describe the complexity of these dynamics. The two-compartment model and the distributed parameter model, both using four free parameters, are examples of high-order perfusion models.

When only limited data are available or the quality of the data is low, it becomes difficult to accurately assess all parameters in high-order models. Simplified models with fewer free parameters are useful in these situations, for example, the extended Toft model (three free parameters). These tracer-kinetic models fix

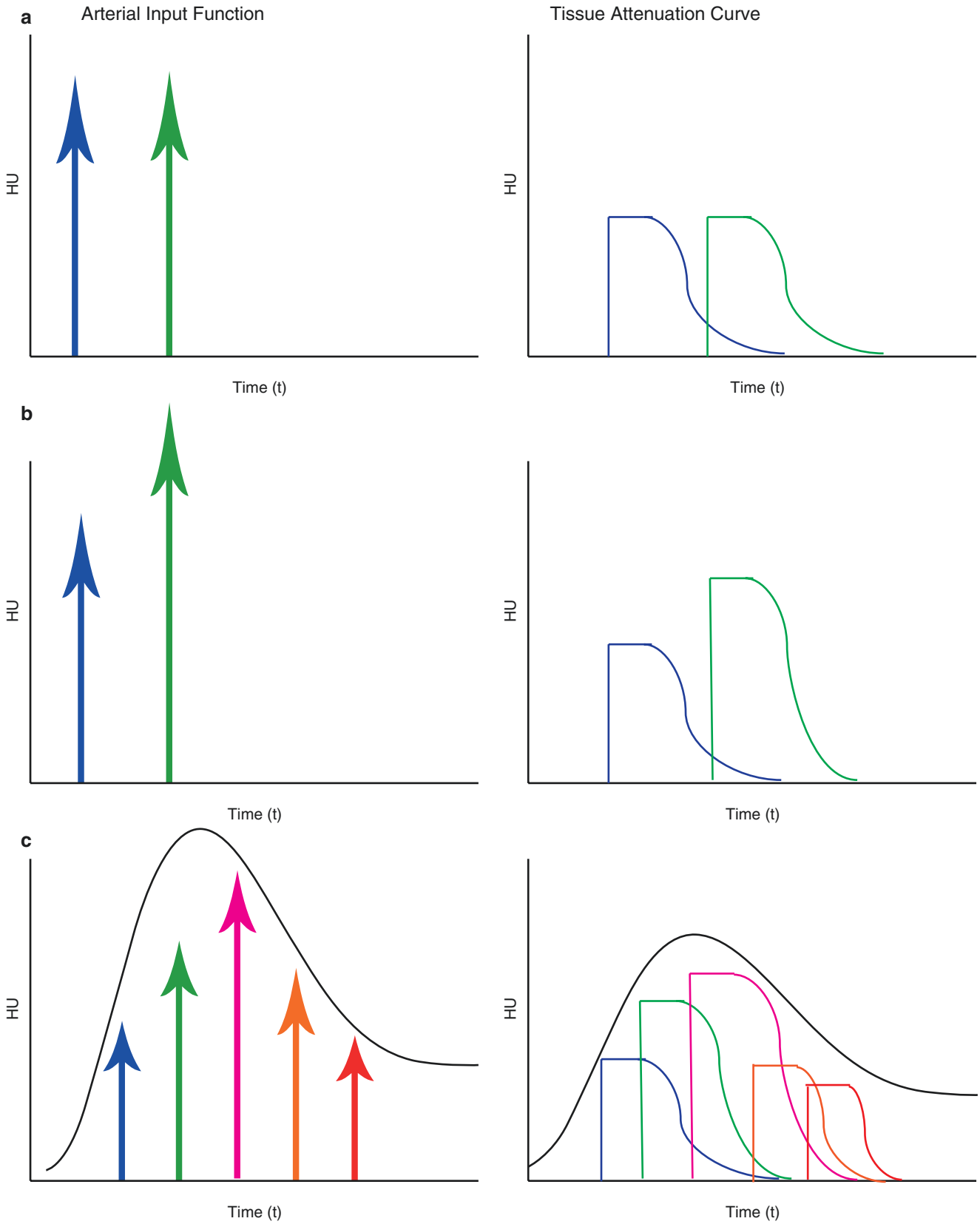

Fig. 63.7 (**a**) When two identical bolus injections of the same concentration (left) are given, then the IRF (right) will be the same for each injection. For each bolus, the IRF shows an abrupt increase in HU values (if the injection is given directly to arterial input); it then stabilizes for a period of time while the bolus passes through the tissue and finally shows a gradual return back to baseline level. The plateau represents the mean transit time. (**b**) When the bolus injections have different properties, for example, different concentrations (left), the corresponding IRFs (right) will be different. (**c**) Contrast medium inflow represented as a series of bolus injections of different concentrations (left) and corresponding IRFs (right). The tissue attenuation curve (TAC) is the sum of all IRFs corresponding to the bolus injections attenuated by the effects of blood flow

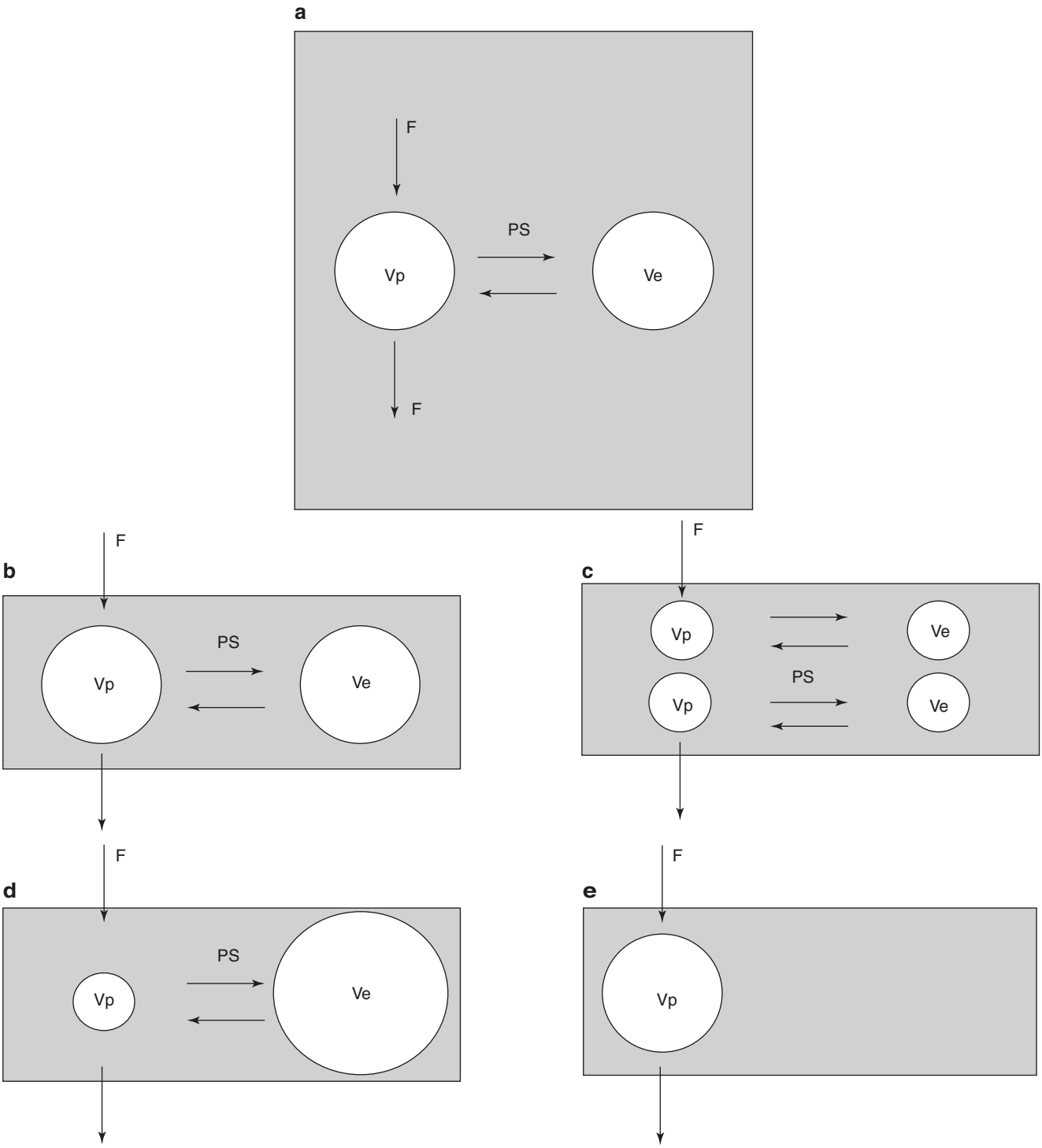

Fig. 63.8 Schematic representation of tracer-kinetic models. (**a**) Schematic representation of the myocardial microcirculation. The **b**lood plasma flows to the vascular space (Vp) driving the myocardial blood flow (F). The Vp compartment exchanges molecules via a flow (PS) with the extracellular extravascular space (Ve). (**b**) Schematics of the two-compartment model. The Vp space can only exchange contrast medium with the Ve space. (**c**) Schematics of the distributed parameter model. The Vp and Ve spaces are represented by multiple small compartments. The contrast medium can only exchange between neighboring compartments. (**d**) Schematics of the extended Toft model, where infinite flow (F) is assumed. (**e**) Schematics of the Fermi model. This mathematical model has only nonphysiological parameters and only the flow (F) can be derived

one (or more) parameters at a constant value resulting in an accurate parameter estimation with less free parameters.

Two-Compartment Model

The two-compartment model describes the intravascular and the extracellular extravascular space as two compartments; see Fig. 63.8b. This model does not take into account the transit times; therefore, the IRF of a two-compartment model does not have a stable plateau as the IRFs in Fig. 63.7. The transit time parameters represent the time a specific amount of blood volume is present in the tissue or capillaries. The peak value of the IRF corresponds to the volume transfer coefficient K_{trans}. This parameter is defined as a product of myocardial blood flow (MBF) and extraction fraction (E) and represents the inflow into the extravascular extracellular space and thereby the delivery of nutrients to tissue.

Patlak Method

This method is used in the majority of dynamic CTMPI patient studies (see Table 63.2) and is a hybrid method based on a two-compartment model combined with the upslope method. In the first phase, the TAC curve is reconstructed from the individual measurements of iodine concentration in the myocardium over time, using a convolution approach. The Patlak method uses a least square fit method to fit a two-compartment model to the TAC curve. Subsequently the MBF is calculated using the upslope method; see Eq. 63.1. The maximal upslope can be derived from the IRF(t) function, describing the TAC curve. Because of the convolution approach to estimate an equation (IRF) describing the TAC, this method is ideal for CT data with low temporal sampling rates where the use of only an upslope method results in inaccurate MBF values because of the limited information on TAC and AIF curves. An example of a low temporal sampling scan mode is the ECG-triggered shuttle mode with a temporal sampling rate of 2–3 s [51].

This method substantially simplifies the mathematical procedures of a model-dependent deconvolution approach. The Volume Perfusion CT (VPCT) myocardium software (MMWP VA41A, Siemens) adopted this method to calculate the MBF in dynamic CTMPI data (Fig. 63.9). Although this

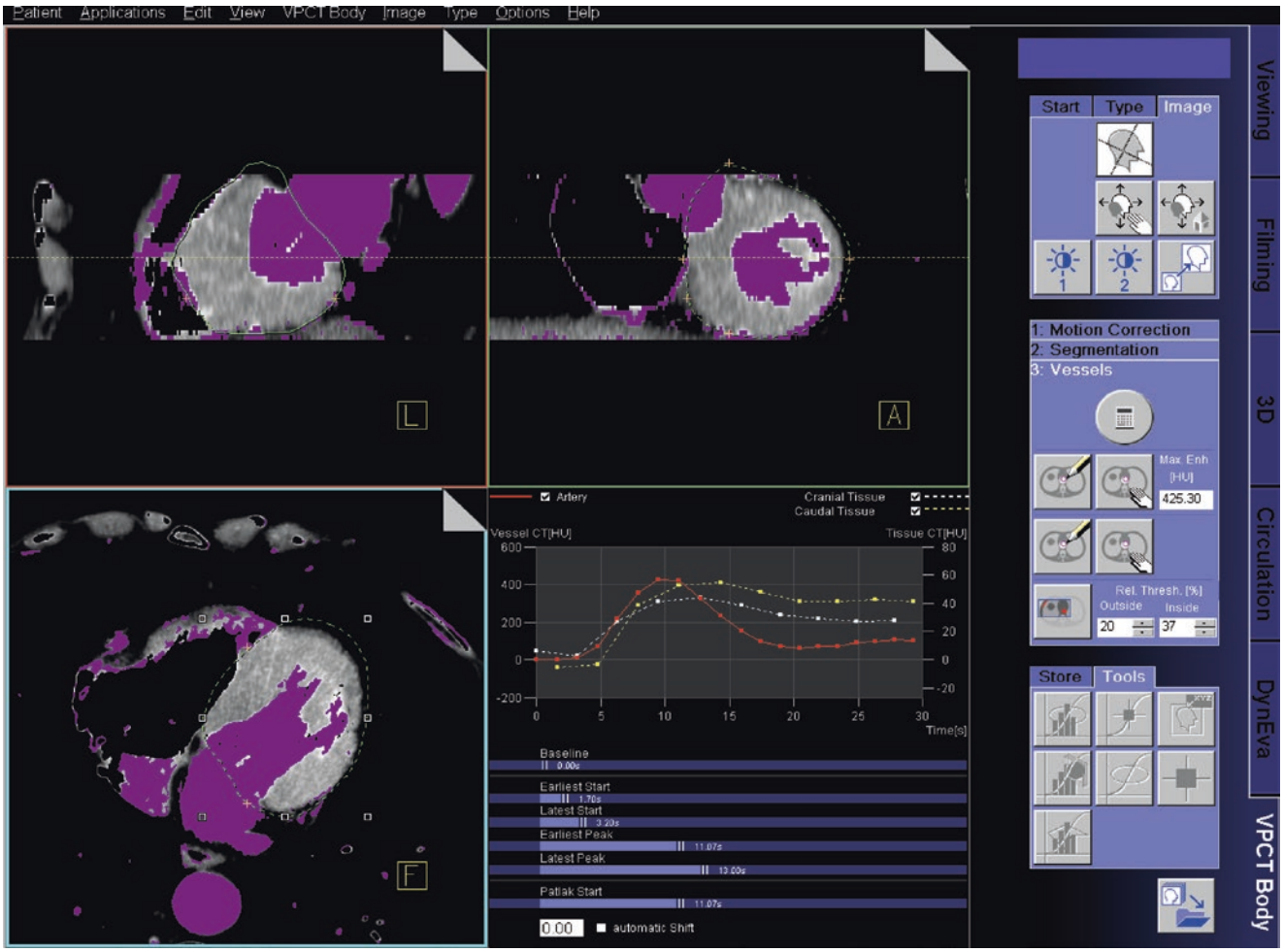

Fig. 63.9 An overview of the Volume Perfusion CT (VPCT) myocardium software (MMWP VA41A, Siemens). Multiple windows allow to visualize different CT axis, show the signal intensity curves for the drawn regions of interest and give corresponding quantitative results

method gives a good estimation and is able to distinguish ischemic myocardium from normal myocardium, MBF is substantially underestimated [16].

More accurate MBF values could be obtained by using Eq. 63.3 to calculate the MBF directly instead of using a hybrid approach with the upslope method (Eq. 63.1). However, this comes at the cost of higher computational complexity.

Distributed Parameter Model

The distributed parameter model is one of the more complex models, taking into account all aspects of contrast medium kinetics. Contrast medium is assumed to exchange between spaces. This model estimates volume, flow, and transit time parameters, providing a full description of the perfusion process [51]. In comparison with other models, the distributed parameter represents both the extracellular extravascular and the vascular space as a series of compartments, Fig. 63.8c. Each extracellular extravascular space compartment interacts only with the nearest vascular space compartment and vice versa. The use of the distributed parameter model is limited by the temporal sampling rate of the CT system. If the temporal sampling rate is too low, accurate estimation of the mean transit times becomes impossible. With higher perfusion flow, the mean transit time decreases, requiring an even higher temporal sampling rate and a compact contrast medium bolus. Because of the complexity of the distributed parameter model, complex fitting methods are required, making the system more susceptible to errors [55]. So et al. [35] used the distributed parameter model to calculate myocardial blood flow using 64-MDCT system. The myocardial perfusion ratio, a ratio between normal and remote myocardium, had 95% sensitivity and 35% specificity to identify ischemic myocardium, with SPECT as reference method.

Extended Toft Model

The extended Toft model has one fixed parameter and three free parameters. It is a simplified variation of the two-compartment model and the distributed parameter model by assuming an infinite flow; see Fig. 63.8d. This means that the MBF cannot be measured with this model; instead the volume transfer coefficient K_{trans} is obtained. Although describing a key part of the perfusion process, this model cannot be used to measure flow and should therefore not be compared to flow-measuring models. However, in situations where the flow cannot be measured accurately due to low temporal sampling rate, the extended Toft model can provide an alternative direct proxy measure for perfusion instead of MBF [51, 55]. So far this model has not been applied in any published dynamic CTMPI study in patients.

Fermi Model

The Fermi model assumes that the contrast medium does not leave the intravascular space. The Fermi model is a mathematical model providing only a functional representation of an IRF. This model does not allow a physiological interpretation of the parameters used in the model; the parameters are simply used as shaping parameters; see Fig. 63.8e. However, the flow (MBF) can still be estimated by the above-described model-dependent deconvolution technique [51, 55]. This model is successfully used in studies on MRI analysis of myocardium perfusion [10, 59–62].

Diagnostic Accuracy

Only a limited number of patient studies (n = 18) has been published on dynamic CTMPI including a total of 805 patients. They are mostly small single-center studies with large inter-study heterogeneity in protocols, scanner type, stressor agent, reference value, analysis method, and cutoff value, making it difficult to compare results.

Visual Analysis

Five studies used visual analysis to evaluate dynamic CTMPI data, including a total of 149 patients with a median of 27 patients per study. These dynamic CTMPI publications using visual analysis are listed in Table 63.1. Sensitivity was found to range from 84% to 98% and specificity from 76% to 98%. All studies with visual analysis of dynamic CT data so far used a second-generation DSCT system.

Two studies analyzed individual segments and two studies analyzed vessel territories. Baxa et al. [22] analyzed both segments and territories. They showed 97% sensitivity and 95% specificity for territory-based analysis, and 98% sensitivity and 96% specificity for segment-based analysis, comparing visual analysis of CTMPI data with ICA. None of the studies performed with visual analysis of dynamic CTMPI data assessed diagnostic accuracy on a per-patient level.

Two visual analysis studies document interobserver agreement between dynamic CTMPI and other perfusion modalities. Weininger et al. [23] compared visual analysis of dynamic CTMPI to SPECT and MRI perfusion and obtained similar results. Interobserver agreement between CTMPI and MRI and CTMPI and SPECT was high with kappa values of 0.85 and 0.82, respectively. Wang et al. [24] compared visual analysis of dynamic CTMPI analysis to SPECT and found high interobserver agreement for detecting perfusion defects with CTMPI and SPECT with kappa values of 0.81 and 0.83, respectively.

Semiquantitative Analysis

Huber et al. [33] is the only study using a semiquantitative parameter (upslope), and they compared it with a quantitative

parameter (linear fit+upslope method) using a 256 row MDCT system with ICA and FFR measurements as a reference standard. The quantitative measured MBF yielded a sensitivity and specificity of 76% and 100%, while the semi-quantitative upslope measure resulted in a reported sensitivity and specificity of 83% and 88%, respectively.

Quantitative Analysis

A total of 13 dynamic CTMPI reports with quantitative analysis are shown in Table 63.2. Included were 656 patients with a median of 37 patients per study. Respective sensitivity and specificity of MBF cutoffs for myocardial ischemia ranged from 73% to 100% and 48% to 100% for MBF. For MBV, sensitivity varied between 75% and 100% and specificity between 24% and 91%. Reference techniques include SPECT, MRI, and ICA + FFR. It should be noted that of these reference techniques only MRI is able to provide a quantitative measure of MBF and MBV values. In studies of Tanabe et al. [26], Huber et al. [33], So et al. [35], and Kido et al. [38], a MDCT system was used; in all other studies, a second-generation DSCT system in shuttle mode was used.

Segment, Territory, and Patient

Bamberg et al. [29, 36] determined the diagnostic accuracy of MBF on segment-, territory-, and patient-based analysis in two separate studies, compared to, respectively, MRI and FFR. Segment-based analysis showed sensitivity of 78% and 91%, respectively, compared to 100% and 93% on territory basis and 100% and 95% on patient basis. Rossi et al. [32] analyzed their MBF data on both per-territory and per-patient level resulting in 88–90% sensitivity and specificity, compared to ICA alone.

Cutoff Values

A wide range of cutoff values (75–103 ml/100 ml/min for MBF) has been proposed to distinguish ischemic from non-ischemic myocardial segments. Studies using DSCT combined with *VPCT* software have reported cutoff values in ml/100 ml/min, while studies using MDCT have reported cutoff values in ml/g/min. Ebersberger et al. [30] used individual cutoff values instead of a generic MBF cutoff value and reported a sensitivity of 86% and a specificity of 96% with SPECT as reference modality. The cutoff values were calculated by subtracting the standard deviation of all segments from the average value of the respective measurement. Kim et al. [63] assessed the range of CTMPI-determined MBF in 19 healthy volunteers in rest and in stress using 128-slice DSCT. Results showed considerable heterogeneity in absolute MBF values. Women had higher MBF values at rest compared to men but had lower MBF values during stress imaging. Danad et al. [64] showed in a myocardial PET perfusion study that gender, age, and weight influence MBF values and that reference MBF values vary significantly within the general population. These results indicate that using a general cutoff value for perfusion parameters may be sub-optimal.

Absolute vs. Relative MBF Values

As mentioned previously, a wide variety of absolute MBF cutoff values have been reported for discriminating ischemic from nonischemic myocardium, as well as a high heterogeneity of MBF values in the normal population. This issue could be avoided by using a relative instead of an absolute measure of MBF. A relative measure comparing normally perfused myocardium with ischemic myocardium may be more accurate for the identification of myocardial ischemia in the individual patient. However, absolute values offer advantage in the diagnosis of global ischemia when normally perfused myocardium is absent.

Wichmann et al. [28] compared absolute MBF values and relative MBF values to CCTA results in 137 patients using a second-generation DSCT. Relative MBF values yielded a higher diagnostic accuracy than absolute MBF values on a territory level, with a sensitivity and specificity of 91% and 93% compared to 82% and 81%. Kono et al. [31] reported similar results in 42 patients using a second-generation DSCT, comparing relative MBF values and absolute MBF values to combined ICA and FFR results. They reported 98% sensitivity and 70% specificity for relative MBF values compared to 89% sensitivity and 48% specificity for absolute MBF values. Both studies used a two-compartment model combined with upslope analysis to calculate MBF.

Myocardial Blood Volume

Myocardial blood volume (MBV) could be another parameter for the detection of myocardial perfusion defects. In ischemic myocardium vasodilation of the arterioles compensates for the decreased flow in the stenotic artery, thereby changing the volume of blood in the myocardium. Bamberg et al. [29] showed that MBV values are lower in infarcted myocardium compared to ischemic myocardium and could therefore help to differentiate between the two states. Three studies evaluated the diagnostic accuracy of both MBF and MBV to detect ischemic myocardium. So et al. [35] used myocardial perfusion reserve (MPR) and myocardial volume reserve (MVR) to detect ischemic areas with SPECT as reference. MPR and MVR were defined as the ratio of MBV and MBF values in stress and rest imaging. They reported sensitivity and specificity of 95% and 35% using MPR, and 97% and 24% using MVR, compared to SPECT results. Ebersberger et al. [30] determined absolute MBF and MBV values and reported a slightly lower sensitivity for MBV than for MBF (81% compared to 86%) with comparable specific-

ity, comparing dynamic CTMPI results to SPECT. Wichmann et al. [27] also determined absolute MBF and MBV values, analyzing one-, two-, or three-vessel territories and compared quantitative analysis of the CTMPI data to visual analysis of perfusion defects of the same CTMPI data. Global MBV values showed lower specificity compared to MBF values. Bamberg et al. [36] compared MBF and MBV values to combined ICA and FFR measurements. They reported that MBF had a significantly higher discriminatory power than MBV to detect myocardial ischemia. The combination of MBF and MBV values was found to be useful in discriminating ischemic and infarcted myocardium from normal myocardium.

Comparison of Visual, Semiquantitative, and Quantitative Analysis

Huber et al. [33] showed a similar diagnostic accuracy for semiquantitative parameters compared to a quantitative measure of MBF in dynamic CTMPI, with combined ICA and FFR results as a reference. The reported sensitivity and specificity were 83% and 88% for the semiquantitative upslope parameter CTMPI, respectively, and 76% and 100% for the quantitative MBF parameter. The range of reported specificities among studies is larger for quantitative analysis, indicating that diagnostic accuracy for a quantitative approach is less robust. However, quantification of myocardial perfusion may be useful in diagnosing three-vessel disease, where there is no nonischemic myocardium present as reference and in the case of global hypoperfusion of the left ventricular myocardium. Three-vessel disease and global hypoperfusion are known to cause false-negative results in SPECT. Meinel et al. [50] investigated whether quantification of global MBF is feasible and showed that global MBF is gradually lower in patients with increasing territorial perfusion defects and is correlated to the number of obstructed vessels. Global MBF showed a moderate correlation with visual CTMPI assessment and CCTA findings [50]. A study of Vliegenthart et al. [9] investigated whether absolute global perfusion parameters as MBF and MBV could detect subclinical changes in perfusion parameters in patients with hypertension and diabetes. This offers the opportunity to use absolute MBF values for the risk stratification of CAD prior to the presence of evident myocardial ischemia. The diagnosis of microvascular disease is another process that could benefit from absolute quantification of MBF with dynamic CTMPI. Microvascular disease is characterized by a decrease in (global) perfusion without correlation to an anatomical abnormality of the coronary arteries. Dynamic CTMPI combined with CTA could possibly be used to diagnose microvascular disease and exclude CAD.

Comparison of Static and Dynamic CTMPI

In an animal study, Schwarz et al. [65] concluded that dynamic CTMPI may be more sensitive for detection of smaller perfusion defects compared to static CTMPI. However, Huber et al. [33] showed that diagnostic accuracy of the dynamic CTMPI parameter was similar to that derived from static CTMPI data using combined ICA and FFR measurements as a reference. More studies are needed to investigate in which patients dynamic CTMPI has additional value beyond visual analysis of myocardial ischemia based on myocardial blood supply imaging.

Comparison with Other Modalities

Currently there are no patient studies comparing dynamic CTMPI and other ischemia imaging modalities against the same reference standard.

Future Perspectives

The limited number of dynamic CTMPI studies in patients shows promising results with regard to the diagnostic value of dynamic CT for the detection of myocardial ischemia. However, several issues need to be addressed before clinical implementation of this technique can be considered.

The currently published patient studies are difficult to compare due to heterogeneity in imaging protocols, reference standards, and analysis techniques. An optimal and robust protocol for dynamic CTMPI is yet to be determined.

The main advantage of dynamic CTMPI compared to other perfusion imaging techniques is the possibility to truly quantify myocardial blood flow, making it possible to accurately identify perfusion defects even in the absence of normally perfused myocardium. Absolute perfusion values offer the possibility of improving CAD risk stratification, diagnosing multivessel CAD, discriminating between infarcted and ischemic myocardium, and identifying early subclinically reduced myocardial perfusion such as in microvascular disease.

Although the quantification of perfusion parameters is assumed to have multiple advantages compared to visual analysis, it is yet to be proven that more accurate MBF (or MBV) values aid in the diagnosis of myocardial ischemia and are able to improve patient outcome. Dynamic CTMPI can be analyzed visually by looking at the dynamic series and quantitatively by either looking at color-coded maps based on absolute values or by analyzing the absolute perfusion parameters directly. Until now there is no study comparing the use of color-coded maps with absolute values to identify ischemic myocardium. The question remains which

of the analysis methods yields highest diagnostic accuracy and best clinical feasibility.

A disadvantage of dynamic CTMPI compared to other modalities is the radiation dose, especially when CCTA and dynamic CTMPI are combined. Patient-tailored protocols to reduce radiation dose should be developed. This could be done by patient-specific tube current and kV modulation and iterative image reconstruction. Static CTMPI is unable to quantify MBF but has a lower radiation dose than dynamic CTMPI. Whether the increased radiation dose of dynamic CTMPI weighs up to the benefits of absolute quantification, and in which patients, is yet to be determined.

Although the main benefit of dynamic CTMPI is the possibility to quantify perfusion, several issues arise with the use of this quantitative imaging method. One of the challenges with dynamic CTMPI is underestimation of MBF compared to other quantitative modalities. Studies with PET-determined MBF [66, 67] have reported stress values between 3 and 5 ml/min/g, whereas dynamic CTMPI studies [24, 32, 36]. report stress MBF values between 1.0 and 1.4 ml/min/g. Studies of Bindschadler et al. [46] and Ishida et al. [16] suggest that a limited temporal sampling rate is the main cause of the underestimation of MBF determined by dynamic CTMPI. Further research should investigate the effect of temporal sampling rate on absolute MBF values and the influence on diagnostic accuracy. A second cause for underestimation of MBF values with dynamic CTMPI could be the use of combining a tracer-kinetic model with the Patlak method to calculate MBF. Possibly this method estimates K_{trans} instead of MBF [16]. By calculating the MBF using a method purely based on deconvolution, MBF values could be more accurate compared to the most widely used hybrid method combining deconvolution and upslope calculation. Each model has its own advantages and disadvantages. Further research is needed to determine which tracer-kinetic model optimally approximates the true value of MBF in CTMPI. Currently, the effect of quantitative perfusion parameters on the diagnostic accuracy in the detection of CAD and myocardial ischemia is still unknown.

There are a few studies comparing the diagnostic accuracy of different perfusion modalities [1, 3]; however, these do not include dynamic CTMPI. The performance of (dynamic) CTMPI with regard to SPECT, PET, and MRI, potentially in combination with anatomical evaluation procedures, needs to be determined in large patient studies including patient outcomes and analysis of cost-effectiveness. Large multicenter studies could also aid in the search for the optimal perfusion cutoff values for several subpopulations in order to increase the diagnostic accuracy. It should be established if dynamic CTMPI in patients with previous coronary artery bypass graft surgery or stent placements has an added value in the diagnostic process. The SPECIFIC study may answer some of these remaining questions. The objective of the multicenter SPECIFIC study is to determine the diagnostic accuracy of CTMPI for the detection of hemodynamically relevant coronary stenosis in patients with suspected or known CAD. A subgroup of patients will also undergo perfusion MRI. The diagnostic accuracy of MRI versus dynamic CTMPI for the detection of perfusion defects will be compared to the reference standard, ICA plus FFR.

In conclusion, the few patient studies focusing on dynamic CTMPI for myocardial ischemia detection show promising results. Absolute quantification of perfusion parameters offers great potential, not only in the diagnosis of myocardial ischemia but potentially also in the detection of early signs of reduced myocardial blood flow as well as the diagnosis of microvascular disease and three-vessel disease. With the advent of new dose reduction techniques and new developments in CT systems, resulting in faster scanning times and wider detectors, clinical implementation of dynamic CTMPI becomes closer.

References

1. Jaarsma C, Leiner T, Bekkers SC, et al. Diagnostic performance of noninvasive myocardial perfusion imaging using single-photon emission computed tomography, cardiac magnetic resonance, and positron emission tomography imaging for the detection of obstructive coronary artery disease. J Am Coll Cardiol. 2012;59(19):1719–28. https://doi.org/10.1016/j.jacc.2011.12.040.
2. Schwitter J, Wacker CM, van Rossum AC, et al. MR-IMPACT: comparison of perfusion-cardiac magnetic resonance with single-photon emission computed tomography for the detection of coronary artery disease in a multicentre, multivendor, randomized trial. Eur Heart J. 2008;29(4):480–9. https://doi.org/10.1093/eurheartj/ehm617.
3. Parker MW, Iskandar A, Limone B, et al. Diagnostic accuracy of cardiac positron emission tomography versus single photon emission computed tomography for coronary artery disease: a bivariate meta-analysis. Circ Cardiovasc Imaging. 2012;5(6):700–7. https://doi.org/10.1161/CIRCIMAGING.112.978270.
4. Hulten EA, Carbonaro S, Petrillo SP, Mitchell JD, Villines TC. Prognostic value of cardiac computed tomography angiography: a systematic review and meta-analysis. J Am Coll Cardiol. 2011;57(10):1237–47. https://doi.org/10.1016/j.jacc.2010.10.011.
5. Pelgrim GJ, Dorrius M, Xie X, et al. The dream of a one-stop-shop: meta-analysis on myocardial perfusion CT. Eur J Radiol. 2015;84(12):2411–20. https://doi.org/10.1016/j.ejrad.2014.12.032.
6. Danad I, Szymonifka J, Schulman-Marcus J, Min JK. Static and dynamic assessment of myocardial perfusion by computed tomography. Eur Hear J Cardiovasc Imaging. 2016;17:836–44. https://doi.org/10.1093/ehjci/jew044.
7. Williams MC, Newby DE. CT myocardial perfusion imaging: current status and future directions. Clin Radiol. 2016;71(8):1–11. https://doi.org/10.1016/j.crad.2016.03.006.
8. Caruso D, Eid M, Schoepf UJ, et al. Dynamic CT myocardial perfusion imaging. Eur J Radiol. 2016;85:1893. https://doi.org/10.1016/j.ejrad.2016.07.017.
9. Vliegenthart R, De Cecco CN, Wichmann JL, et al. Dynamic CT myocardial perfusion imaging identifies early perfusion abnormalities in diabetes and hypertension: insights from a multicenter registry. J Cardiovasc Comput Tomogr. 2016;10(4):301–8. https://doi.org/10.1016/j.jcct.2016.05.005.

10. George RT, Jerosch-Herold M, Silva C, et al. Quantification of myocardial perfusion using dynamic 64-detector computed tomography. Investig Radiol. 2007;42(12):815–22. https://doi.org/10.1097/RLI.0b013e318124a884.
11. Christian TF, Frankish ML, Sisemoore JH, et al. Myocardial perfusion imaging with first-pass computed tomographic imaging: measurement of coronary flow reserve in an animal model of regional hyperemia. J Nucl Cardiol. 2010;17(4):625–30. https://doi.org/10.1007/s12350-010-9206-6.
12. So A, Hsieh J, Li J-Y, Hadway J, Kong H-F, Lee T-Y. Quantitative myocardial perfusion measurement using CT perfusion: a validation study in a porcine model of reperfused acute myocardial infarction. Int J Cardiovasc Imaging. 2012;28(5):1237–48. https://doi.org/10.1007/s10554-011-9927-x.
13. Mahnken AH, Klotz E, Pietsch H, et al. Quantitative whole heart stress perfusion CT imaging as noninvasive assessment of hemodynamics in coronary artery stenosis: preliminary animal experience. Investig Radiol. 2010;45(6):298–305. https://doi.org/10.1097/RLI.0b013e3181dfa3cf.
14. Bamberg F, Hinkel R, Schwarz F, Sandner TA, Baloch E, Marcus R, Becker A, Kupatt C, Wintersperger BJ, Johnson TR, Theisen DKM. Accuracy of dynamic computed tomography adenosine stress myocardial perfusion imaging in estimating myocardial blood flow at various degrees of coronary artery stenosis using a porcine animal model. Investig Radiol. 2012;47(1):71–7.
15. Rossi A, Uitterdijk A, Dijkshoorn M, et al. Quantification of myocardial blood flow by adenosine-stress CT perfusion imaging in pigs during various degrees of stenosis correlates well with coronary artery blood flow and fractional flow reserve. Eur Heart J Cardiovasc Imaging. 2013;14(4):331–8. https://doi.org/10.1093/ehjci/jes150.
16. Ishida M, Kitagawa K, Ichihara T, et al. Underestimation of myocardial blood flow by dynamic perfusion CT: explanations by two-compartment model analysis and limited temporal sampling of dynamic CT. J Cardiovasc Comput Tomogr. 2016;10:1–8. https://doi.org/10.1016/j.jcct.2016.01.008.
17. Motwani M, Fairbairn TA, Larghat A, et al. Systolic versus diastolic acquisition in myocardial perfusion MR imaging. Radiology. 2012;262(3):816–23. https://doi.org/10.1148/radiol.11111549.
18. Motwani M, Kidambi A, Sourbron S, et al. Quantitative three-dimensional cardiovascular magnetic resonance myocardial perfusion imaging in systole and diastole at 3.0 T. Heart. 2013;99:A56–7. https://doi.org/10.1186/1532-429X-16-19.
19. Rossi A, Merkus D, Klotz E, Mollet N, de Feyter PJ, Krestin GP. Stress myocardial perfusion: imaging with multidetector CT. Radiology. 2014;270(1):25–46. https://doi.org/10.1148/radiol.13112739.
20. Einstein AJ. Effects of radiation exposure from cardiac imaging: how good. J Am College Cardiol. 2012;59(6):553–65. https://doi.org/10.1016/j.jacc.2011.08.079.Effects.
21. Yang DH, Kim Y-H, Roh JH, et al. Diagnostic performance of on-site CT-derived fractional flow reserve versus CT perfusion. Eur Heart J Cardiovasc Imaging. 2016;18:432. https://doi.org/10.1093/ehjci/jew094.
22. Baxa J, Hromádka M, Šedivý J, et al. Regadenoson-stress dynamic myocardial perfusion improves diagnostic performance of CT angiography in assessment of intermediate coronary artery stenosis in asymptomatic patients. Biomed Res Int. 2015;2015:105629. https://doi.org/10.1155/2015/105629.
23. Weininger M, Schoepf UJ, Ramachandra A, et al. Adenosine-stress dynamic real-time myocardial perfusion CT and adenosine-stress first-pass dual-energy myocardial perfusion CT for the assessment of acute chest pain: initial results. Eur J Radiol. 2012;81(12):3703–10. https://doi.org/10.1016/j.ejrad.2010.11.022.
24. Wang Y, Qin L, Shi X, et al. Adenosine-stress dynamic myocardial perfusion imaging with second-generation dual-source CT: comparison with conventional catheter coronary angiography and SPECT nuclear myocardial perfusion imaging. Am J Roentgenol. 2012;198(3):521–9. https://doi.org/10.2214/AJR.11.7830.
25. Bastarrika G, Ramos-Duran L, Rosenblum MA, Kang DK, Rowe GW, Schoepf UJ. Adenosine-stress dynamic myocardial CT perfusion imaging: initial clinical experience. Investig Radiol. 2010;45(6):306–13. https://doi.org/10.1097/RLI.0b013e3181dfa2f2.
26. Tanabe Y, Kido T, Uetani T, et al. Differentiation of myocardial ischemia and infarction assessed by dynamic computed tomography perfusion imaging and comparison with cardiac magnetic resonance and single-photon emission computed tomography. Eur Radiol. 2016:1–12. http://www.embase.com/search/results?subaction=viewrecord&from=export&id=L608199060.
27. Wichmann JL, Meinel FG, Schoepf UJ, et al. Semiautomated global quantification of left ventricular myocardial perfusion at stress dynamic ct: diagnostic accuracy for detection of territorial myocardial perfusion deficits compared to visual assessment. Acad Radiol. 2016;23(4):429–37. https://doi.org/10.1016/j.acra.2015.12.005.
28. Wichmann JL, Meinel FG, Schoepf UJ, et al. Absolute versus relative myocardial blood flow by dynamic CT myocardial perfusion imaging in patients with anatomic coronary artery disease. Am J Roentgenol. 2015;205(1):W67–72. https://doi.org/10.2214/AJR.14.14087.
29. Bamberg F, Marcus RP, Becker A, et al. Dynamic myocardial CT perfusion imaging for evaluation of myocardial ischemia as determined by MR imaging. JACC Cardiovasc Imaging. 2014;7(3):267–77. https://doi.org/10.1016/j.jcmg.2013.06.008.
30. Ebersberger U, Marcus RP, Schoepf UJ, et al. Dynamic CT myocardial perfusion imaging: performance of 3D semi-automated evaluation software. Eur Radiol. 2014;24(1):191–9. https://doi.org/10.1007/s00330-013-2997-5.
31. Kono AK, Coenen A, Lubbers M, et al. Relative myocardial blood flow by dynamic computed tomographic perfusion imaging predicts hemodynamic significance of coronary stenosis better than absolute blood flow. Investig Radiol. 2014;49(12):801–7. https://doi.org/10.1097/RLI.0000000000000087.
32. Rossi A, Dharampal A, Wragg A, et al. Diagnostic performance of hyperaemic myocardial blood flow index obtained by dynamic computed tomography: does it predict functionally significant coronary lesions? Eur Heart J Cardiovasc Imaging. 2014;15(1):85–94. https://doi.org/10.1093/ehjci/jet133.
33. Huber AM, Leber V, Gramer BM, et al. Myocardium: dynamic versus single-shot CT perfusion imaging. Radiology. 2013;269(2):1–8. https://doi.org/10.1148/radiol.13121441.
34. Greif M, von Ziegler F, Bamberg F, et al. CT stress perfusion imaging for detection of haemodynamically relevant coronary stenosis as defined by FFR. Heart. 2013;99(14):1004–11. https://doi.org/10.1136/heartjnl-2013-303794.
35. So A, Wisenberg G, Islam A, et al. Non-invasive assessment of functionally relevant coronary artery stenoses with quantitative CT perfusion: preliminary clinical experiences. Eur Radiol. 2012;22(1):39–50. https://doi.org/10.1007/s00330-011-2260-x.
36. Bamberg F, Becker A, Schwarz F, et al. Detection of hemodynamically significant coronary artery stenosis : incremental diagnostic value of dynamic CT-based. Radiology. 2011;260(3):689–98. https://doi.org/10.1148/radiol.11110638/-/DC1.
37. Ho KT, Chua KC, Klotz E, Panknin C. Stress and rest dynamic myocardial perfusion imaging by evaluation of complete time-attenuation curves with dual-source CT. JACC Cardiovasc Imaging. 2010;3(8):811–20. https://doi.org/10.1016/j.jcmg.2010.05.009.
38. Kido T, Kurata A, Higashino H, Inoue Y. Quantification of regional myocardial blood flow using. Circ J. 2008;72:1086–91.
39. Kim SM, Kim YN, Choe YH. Adenosine-stress dynamic myocardial perfusion imaging using 128-slice dual-source CT: optimization of the CT protocol to reduce the radiation dose. Int J

Cardiovasc Imaging. 2013;29(4):875–84. https://doi.org/10.1007/s10554-012-0138-x.
40. Deseive S, Pugliese Md F, Meave A, et al. Image quality and radiation dose of a prospectively electrocardiography-triggered high-pitch data acquisition strategy for coronary CT angiography: the multicenter, randomized PROTECTION IV study. J Cardiovasc Comput Tomogr. 2015;9:278–85. https://doi.org/10.1016/j.jcct.2015.03.001.
41. Gordic S, Desbiolles L, Sedlmair M, et al. Optimizing radiation dose by using advanced modelled iterative reconstruction in high-pitch coronary CT angiography. Eur Radiol. 2016;26(2):459–68. https://doi.org/10.1007/s00330-015-3862-5.
42. Einstein AJ, Moser KW, Thompson RC, Cerqueira MD, Henzlova MJ. Radiation dose to patients from cardiac diagnostic imaging. Circulation. 2007;116(11):1290–305. https://doi.org/10.1161/CIRCULATIONAHA.107.688101.
43. Danad I, Raijmakers PG, Appelman YE, et al. Hybrid imaging using quantitative H215O PET and CT-based coronary angiography for the detection of coronary artery disease. J Nucl Med. 2013;54(1):55–63. https://doi.org/10.2967/jnumed.112.104687.
44. Fujita M, Kitagawa K, Ito T, et al. Dose reduction in dynamic CT stress myocardial perfusion imaging: comparison of 80-kV/370-mAs and 100-kV/300-mAs protocols. Eur Radiol. 2014;24(3):748–55. https://doi.org/10.1007/s00330-013-3063-z.
45. Gramer BM, Muenzel D, Leber V, et al. Impact of iterative reconstruction on CNR and SNR in dynamic myocardial perfusion imaging in an animal model. Eur Radiol. 2012;22(12):2654–61. https://doi.org/10.1007/s00330-012-2525-z.
46. Bindschadler M, Modgil D, Branch KR, La Riviere PJ, Alessio AM. Comparison of blood flow models and acquisitions for quantitative myocardial perfusion estimation from dynamic CT. Phys Med Biol. 2008;141(4):520–9. https://doi.org/10.1016/j.surg.2006.10.010.Use.
47. Zoghbi GJ, Dorfman TA, Iskandrian AE. The effects of medications on myocardial perfusion. J Am Coll Cardiol. 2008;52(6):401–16. https://doi.org/10.1016/j.jacc.2008.04.035.
48. Machecourt J, Longère P, Fagret D, et al. Prognostic value of thallium-201 single-photon emission computed tomographic myocardial perfusion imaging according to extent of myocardial defect. Study in 1,926 patients with foilow-up at 33 months. J Am Coll Cardiol. 1994;23(5):1096–106. https://doi.org/10.1016/0735-1097(94)90597-5.
49. Cerqueira MD, Weissman NJ, Dilsizian V, et al. Standardized myocardial segmentation and nomenclature for tomographic imaging of the heart. Circulation. 2002;105:539–42.
50. Meinel FG, Ebersberger U, Schoepf UJ, et al. Global quantification of left ventricular myocardial perfusion at dynamic CT: feasibility in a multicenter patient population. Am J Roentgenol. 2014;203(2):174–80. https://doi.org/10.2214/AJR.13.12328.
51. Ingrisch M, Sourbron S. Tracer-kinetic modeling of dynamic contrast-enhanced MRI and CT: a primer. J Pharmacokinet Pharmacodyn. 2013;40(3, SI):281–300. https://doi.org/10.1007/s10928-013-9315-3.
52. Al-Saadi N, Nagel E, Gross M, et al. Noninvasive detection of myocardial ischemia from perfusion reserve based on cardiovascular magnetic resonance. Circulation. 2000;101(12):1379–83.
53. Al-Saadi N, Nagel E, Gross M, et al. Improvement of myocardial perfusion reserve early after coronary intervention: assessment with cardiac magnetic resonance imaging. J Am Coll Cardiol. 2000;36(5):1557–64.
54. Schwitter J, Nanz D, Kneifel S, et al. Assessment of myocardial perfusion in coronary artery disease by magnetic resonance: a comparison with positron emission tomography and coronary angiography. Circulation. 2001;103(18):2230–5.
55. Pelgrim G, Handayani A, Dijkstra H, et al. Quantitative myocardial perfusion with dynamic contrast-enhanced imaging in MRI and CT : theoretical models and current implementation. Biomed Res Int. 2016;2016:1.
56. Lee TY. Functional CT: physiological models. Trends Biotechnol. 2002;20(8):3–10. https://doi.org/10.1016/S0167-7799(02)02035-8.
57. Larghat AM, Maredia N, Biglands J, et al. Reproducibility of first-pass cardiovascular magnetic resonance myocardial perfusion. J Magn Reson Imaging. 2013;37(4):865–74. https://doi.org/10.1002/jmri.23889.
58. Gamel BJ, Katholi CR, Mesel E. Pitfalls in digital computation of the impulse response of vascular beds from indicator-dilution curves. Circ Res. 1973;32(April):516–23.
59. Papanastasiou G, Williams MC, Kershaw LE, et al. Measurement of myocardial blood flow by cardiovascular magnetic resonance perfusion: comparison of distributed parameter and Fermi models with single and dual bolus. J Cardiovasc Magn Reson. 2015;17:17. https://doi.org/10.1186/s12968-015-0125-1.
60. Futamatsu H, Wilke N, Klassen C, et al. Evaluation of cardiac magnetic resonance imaging parameters to detect anatomically and hemodynamically significant coronary artery disease. Am Heart J. 2007;154(2):298–305. https://doi.org/10.1016/j.ahj.2007.04.024.
61. Maredia N, Plein S, Younger JF, et al. Detection of triple vessel coronary artery disease by visual and quantitative first pass CMR myocardial perfusion imaging in the CE-MARC study. J Cardiovasc Magn Reson. 2011;13. http://www.embase.com/search/results?subaction=viewrecord&from=export&id=L70465436:O29.
62. Sammut E, Zarinabad N, Wesolowski R, et al. Feasibility of high-resolution quantitative perfusion analysis in patients with heart failure. J Cardiovasc Magn Reson. 2015;17:13. https://doi.org/10.1186/s12968-015-0124-2.
63. Kim EY, Chung WJ, Sung YM, et al. Normal range and regional heterogeneity of myocardial perfusion in healthy human myocardium: assessment on dynamic perfusion CT using 128-slice dual-source CT. Int J Cardiovasc Imaging. 2014;30(SUPPL. 1):33–40. https://doi.org/10.1007/s10554-014-0432-x.
64. Danad I, Raijmakers PG, Appelman YE, et al. Coronary risk factors and myocardial blood flow in patients evaluated for coronary artery disease: a quantitative [15O]H2O PET/CT study. Eur J Nucl Med Mol Imaging. 2012;39(1):102–12. https://doi.org/10.1007/s00259-011-1956-0.
65. Schwarz F, Hinkel R, Baloch E, et al. Myocardial CT perfusion imaging in a large animal model: comparison of dynamic versus single-phase acquisitions. JACC Cardiovasc Imaging. 2013;6(12):1229–38. https://doi.org/10.1016/j.jcmg.2013.05.018.
66. Kajander SA, Joutsiniemi E, Saraste M, et al. Clinical value of absolute quantification of myocardial perfusion with (15)O-water in coronary artery disease. Circ Cardiovasc Imaging. 2011;4(6):678–84. https://doi.org/10.1161/CIRCIMAGING.110.960732.
67. Bol A, Melin JA, Vanoverschelde JL, et al. Direct comparison of [13N]ammonia and [15O]water estimates of perfusion with quantification of regional myocardial blood flow by microspheres. Circulation. 1993;87(2):512–25. https://doi.org/10.1161/01.CIR.87.2.512.